

Measurements of Higher Order Flow Harmonics in Au + Au Collisions at $\sqrt{s_{NN}} = 200$ GeV

A. Adare,¹¹ S. Afanasiev,²⁷ C. Aidala,⁴⁰ N.N. Ajitanand,⁵⁷ Y. Akiba,^{51,52} H. Al-Bataineh,⁴⁶ J. Alexander,⁵⁷ K. Aoki,^{33,51} Y. Aramaki,¹⁰ E. T. Atomssa,³⁴ R. Averbeck,⁵⁸ T. C. Awes,⁴⁷ B. Azmoun,⁵ V. Babintsev,²² M. Bai,⁴ G. Baksay,¹⁸ L. Baksay,¹⁸ K. N. Barish,⁶ B. Bassalleck,⁴⁵ A. T. Basye,¹ S. Bathe,⁶ V. Baublis,⁵⁰ C. Baumann,⁴¹ A. Bazilevsky,⁵ S. Belikov,^{5,*} R. Belmont,⁶² R. Bennett,⁵⁸ A. Berdnikov,⁵⁴ Y. Berdnikov,⁵⁴ A. A. Bickley,¹¹ J. S. Bok,⁶⁵ K. Boyle,⁵⁸ M. L. Brooks,³⁶ H. Buesching,⁵ V. Bumazhnov,²² G. Bunce,^{5,52} S. Butsyk,³⁶ C. M. Camacho,³⁶ S. Campbell,⁵⁸ C.-H. Chen,⁵⁸ C. Y. Chi,¹² M. Chiu,⁵ I. J. Choi,⁶⁵ R. K. Choudhury,³ P. Christiansen,³⁸ T. Chujo,⁶¹ P. Chung,⁵⁷ O. Chvala,⁶ V. Cianciolo,⁴⁷ Z. Citron,⁵⁸ B. A. Cole,¹² M. Connors,⁵⁸ P. Constantin,³⁶ M. Csanád,¹⁶ T. Csörgő,³⁰ T. Dahms,⁵⁸ S. Dairaku,^{33,51} I. Danchev,⁶² K. Das,¹⁹ A. Datta,⁴⁰ G. David,⁵ A. Denisov,²² A. Deshpande,^{52,58} E. J. Desmond,⁵ O. Dietzsch,⁵⁵ A. Dion,⁵⁸ M. Donadelli,⁵⁵ O. Drapier,³⁴ A. Drees,⁵⁸ K. A. Drees,⁴ J. M. Durham,⁵⁸ A. Durum,²² D. Dutta,³ S. Edwards,¹⁹ Y. V. Efremenko,⁴⁷ F. Ellinghaus,¹¹ T. Engelmore,¹² A. Enokizono,³⁵ H. En'yo,^{51,52} S. Esumi,⁶¹ B. Fadem,⁴² D. E. Fields,⁴⁵ M. Finger,⁷ M. Finger, Jr.,⁷ F. Fleuret,³⁴ S. L. Fokin,³² Z. Fraenkel,^{64,*} J. E. Frantz,⁵⁸ A. Franz,⁵ A. D. Frawley,¹⁹ K. Fujiwara,⁵¹ Y. Fukao,⁵¹ T. Fusayasu,⁴⁴ I. Garishvili,⁵⁹ A. Glenn,¹¹ H. Gong,⁵⁸ M. Gonin,³⁴ Y. Goto,^{51,52} R. Granier de Cassagnac,³⁴ N. Grau,¹² S. V. Greene,⁶² M. Grosse Perdekamp,^{23,52} T. Gunji,¹⁰ H.-Å. Gustafsson,^{38,*} J. S. Haggerty,⁵ K. I. Hahn,¹⁷ H. Hamagaki,¹⁰ J. Hamblen,⁵⁹ R. Han,⁴⁹ J. Hanks,¹² E. P. Hartouni,³⁵ E. Haslum,³⁸ R. Hayano,¹⁰ X. He,²⁰ M. Heffner,³⁵ T. K. Hemmick,⁵⁸ T. Hester,⁶ J. C. Hill,²⁶ M. Hohlmann,¹⁸ W. Holzmann,¹² K. Homma,²¹ B. Hong,³¹ T. Horaguchi,²¹ D. Hornback,⁵⁹ S. Huang,⁶² T. Ichihara,^{51,52} R. Ichimiya,⁵¹ J. Ide,⁴² Y. Ikeda,⁶¹ K. Imai,^{33,51} M. Inaba,⁶¹ D. Isenhower,¹ M. Ishihara,⁵¹ T. Isobe,^{10,51} M. Issah,⁶² A. Isupov,²⁷ D. Ivanishev,⁵⁰ B. V. Jacak,^{58,†} J. Jia,^{5,57} J. Jin,¹² B. M. Johnson,⁵ K. S. Joo,⁴³ D. Jouan,⁴⁸ D. S. Jumper,¹ F. Kajihara,¹⁰ S. Kametani,⁵¹ N. Kamihara,⁵² J. Kamin,⁵⁸ J. H. Kang,⁶⁵ J. Kapustinsky,³⁶ K. Karatsu,^{33,51} D. Kawall,^{40,52} M. Kawashima,^{53,51} A. V. Kazantsev,³² T. Kempel,²⁶ A. Khanzadeev,⁵⁰ K. M. Kijima,²¹ B. I. Kim,³¹ D. H. Kim,⁴³ D. J. Kim,²⁸ E. Kim,⁵⁶ E. J. Kim,⁸ S. H. Kim,⁶⁵ Y. J. Kim,²³ E. Kinney,¹¹ K. Kiriluk,¹¹ Á. Kiss,¹⁶ E. Kistenev,⁵ L. Kochenda,⁵⁰ B. Komkov,⁵⁰ M. Konno,⁶¹ J. Koster,²³ D. Kotchetkov,⁴⁵ A. Kozlov,⁶⁴ A. Král,¹³ A. Kravitz,¹² G. J. Kunde,³⁶ K. Kurita,^{53,51} M. Kurosawa,⁵¹ Y. Kwon,⁶⁵ G. S. Kyle,⁴⁶ R. Lacey,⁵⁷ Y. S. Lai,¹² J. G. Lajoie,²⁶ A. Lebedev,²⁶ D. M. Lee,³⁶ J. Lee,¹⁷ K. Lee,⁵⁶ K. B. Lee,³¹ K. S. Lee,³¹ M. J. Leitch,³⁶ M. A. L. Leite,⁵⁵ E. Leitner,⁶² B. Lenzi,⁵⁵ X. Li,⁹ P. Liebing,⁵² L. A. Linden Levy,¹¹ T. Liška,¹³ A. Litvinenko,²⁷ H. Liu,^{36,46} M. X. Liu,³⁶ B. Love,⁶² R. Luechtenborg,⁴¹ D. Lynch,⁵ C. F. Maguire,⁶² Y. I. Makdisi,⁴ A. Malakhov,²⁷ M. D. Malik,⁴⁵ V. I. Manko,³² E. Mannel,¹² Y. Mao,^{49,51} H. Masui,⁶¹ F. Matathias,¹² M. McCumber,⁵⁸ P. L. McGaughey,³⁶ N. Means,⁵⁸ B. Meredith,²³ Y. Miake,⁶¹ A. C. Mignerey,³⁹ P. Mikeš,^{7,25} K. Miki,^{61,51} A. Milov,⁵ M. Mishra,² J. T. Mitchell,⁵ A. K. Mohanty,³ Y. Morino,¹⁰ A. Morreale,⁶ D. P. Morrison,⁵ T. V. Moukhanova,³² J. Murata,^{53,51} S. Nagamiya,²⁹ J. L. Nagle,¹¹ M. Naglis,⁶⁴ M. I. Nagy,¹⁶ I. Nakagawa,^{51,52} Y. Nakamiya,²¹ T. Nakamura,^{21,29} K. Nakano,^{51,60} J. Newby,³⁵ M. Nguyen,⁵⁸ R. Nouicer,⁵ A. S. Nyanin,³² E. O'Brien,⁵ S. X. Oda,¹⁰ C. A. Ogilvie,²⁶ M. Oka,⁶¹ K. Okada,⁵² Y. Onuki,⁵¹ A. Oskarsson,³⁸ M. Ouchida,^{21,51} K. Ozawa,¹⁰ R. Pak,⁵ V. Pantuev,^{24,58} V. Papavassiliou,⁴⁶ I. H. Park,¹⁷ J. Park,⁵⁶ S. K. Park,³¹ W. J. Park,³¹ S. F. Pate,⁴⁶ H. Pei,²⁶ J.-C. Peng,²³ H. Pereira,¹⁴ V. Peresedov,²⁷ D. Yu. Peressounko,³² C. Pinkenburg,⁵ R. P. Pisani,⁵ M. Proissl,⁵⁸ M. L. Purschke,⁵ A. K. Purwar,³⁶ H. Qu,²⁰ J. Rak,²⁸ A. Rakotozafindrabe,³⁴ I. Ravinovich,⁶⁴ K. F. Read,^{47,59} K. Reygers,⁴¹ V. Riabov,⁵⁰ Y. Riabov,⁵⁰ E. Richardson,³⁹ D. Roach,⁶² G. Roche,³⁷ S. D. Rolnick,⁶ M. Rosati,²⁶ C. A. Rosen,¹¹ S. S. E. Rosendahl,³⁸ P. Rosnet,³⁷ P. Rukoyatkin,²⁷ P. Ružička,²⁵ B. Sahlmueller,⁴¹ N. Saito,²⁹ T. Sakaguchi,⁵ K. Sakashita,^{51,60} V. Samsonov,⁵⁰ S. Sano,^{10,63} T. Sato,⁶¹ S. Sawada,²⁹ K. Sedgwick,⁶ J. Seele,¹¹ R. Seidl,²³ A. Yu. Semenov,²⁶ R. Seto,⁶ D. Sharma,⁶⁴ I. Shein,²² T.-A. Shibata,^{51,60} K. Shigaki,²¹ M. Shimomura,⁶¹ K. Shoji,^{33,51} P. Shukla,³ A. Sickles,⁵ C. L. Silva,⁵⁵ D. Silvermyr,⁴⁷ C. Silvestre,¹⁴ K. S. Sim,³¹ B. K. Singh,² C. P. Singh,² V. Singh,² M. Slunečka,⁷ R. A. Soltz,³⁵ W. E. Sondheim,³⁶ S. P. Sorensen,⁵⁹ I. V. Sourikova,⁵ N. A. Sparks,¹ P. W. Stankus,⁴⁷ E. Stenlund,³⁸ S. P. Stoll,⁵ T. Sugitate,²¹ A. Sukhanov,⁵ J. Sziklai,³⁰ E. M. Takagui,⁵⁵ A. Taketani,^{51,52} R. Tanabe,⁶¹ Y. Tanaka,⁴⁴ K. Tanida,^{33,51,52} M. J. Tannenbaum,⁵ S. Tarafdar,² A. Taranenko,⁵⁷ P. Tarján,¹⁵ H. Themann,⁵⁸ T. L. Thomas,⁴⁵ M. Togawa,^{33,51} A. Toia,⁵⁸ L. Tomášek,²⁵ H. Torii,²¹ R. S. Towell,¹ I. Tserruya,⁶⁴ Y. Tsuchimoto,²¹ C. Vale,^{5,26} H. Valle,⁶² H. W. van Hecke,³⁶ E. Vazquez-Zambrano,¹² A. Veicht,²³ J. Velkova,⁶² R. Vértesi,^{15,30} A. A. Vinogradov,³² M. Virius,¹³ V. Vrba,²⁵ E. Vznuzdaev,⁵⁰ X. R. Wang,⁴⁶ D. Watanabe,²¹ K. Watanabe,⁶¹ Y. Watanabe,^{51,52} F. Wei,²⁶ R. Wei,⁵⁷ J. Wessels,⁴¹ S. N. White,⁵ D. Winter,¹² J. P. Wood,¹ C. L. Woody,⁵ R. M. Wright,¹ M. Wysocki,¹¹ W. Xie,⁵² Y. L. Yamaguchi,¹⁰ K. Yamaura,²¹ R. Yang,²³ A. Yanovich,²² J. Ying,²⁰ S. Yokkaichi,^{51,52} Z. You,⁴⁹ G. R. Young,⁴⁷ I. Younus,⁴⁵ I. E. Yushmanov,³² W. A. Zajc,¹² C. Zhang,⁴⁷ S. Zhou,⁹ and L. Zolin²⁷

(PHENIX Collaboration)

- ¹Abilene Christian University, Abilene, Texas 79699, USA
²Department of Physics, Banaras Hindu University, Varanasi 221005, India
³Bhabha Atomic Research Centre, Bombay 400 085, India
⁴Collider-Accelerator Department, Brookhaven National Laboratory, Upton, New York 11973-5000, USA
⁵Physics Department, Brookhaven National Laboratory, Upton, New York 11973-5000, USA
⁶University of California-Riverside, Riverside, California 92521, USA
⁷Charles University, Ovocný trh 5, Praha 1, 116 36, Prague, Czech Republic
⁸Chonbuk National University, Jeonju, 561-756, Korea
⁹Science and Technology on Nuclear Data Laboratory, China Institute of Atomic Energy, Beijing 102413, P. R. China
¹⁰Center for Nuclear Study, Graduate School of Science, University of Tokyo, 7-3-1 Hongo, Bunkyo, Tokyo 113-0033, Japan
¹¹University of Colorado, Boulder, Colorado 80309, USA
¹²Columbia University, New York, New York 10027 and Nevis Laboratories, Irvington, New York 10533, USA
¹³Czech Technical University, Zikova 4, 166 36 Prague 6, Czech Republic
¹⁴Dapnia, CEA Saclay, F-91191, Gif-sur-Yvette, France
¹⁵Debrecen University, H-4010 Debrecen, Egyetem tér 1, Hungary
¹⁶ELTE, Eötvös Loránd University, H-1117 Budapest, Pázmány P. s. 1/A, Hungary
¹⁷Ewha Womans University, Seoul 120-750, Korea
¹⁸Florida Institute of Technology, Melbourne, Florida 32901, USA
¹⁹Florida State University, Tallahassee, Florida 32306, USA
²⁰Georgia State University, Atlanta, Georgia 30303, USA
²¹Hiroshima University, Kagamiyama, Higashi-Hiroshima 739-8526, Japan
²²IHEP Protvino, State Research Center of Russian Federation, Institute for High Energy Physics, Protvino, 142281, Russia
²³University of Illinois at Urbana-Champaign, Urbana, Illinois 61801, USA
²⁴Institute for Nuclear Research of the Russian Academy of Sciences, prospekt 60-letiya Oktyabrya 7a, Moscow 117312, Russia
²⁵Institute of Physics, Academy of Sciences of the Czech Republic, Na Slovance 2, 182 21 Prague 8, Czech Republic
²⁶Iowa State University, Ames, Iowa 50011, USA
²⁷Joint Institute for Nuclear Research, 141980 Dubna, Moscow Region, Russia
²⁸Helsinki Institute of Physics and University of Jyväskylä, P. O. Box 35, FI-40014 Jyväskylä, Finland
²⁹KEK, High Energy Accelerator Research Organization, Tsukuba, Ibaraki 305-0801, Japan
³⁰KFKI Research Institute for Particle and Nuclear Physics of the Hungarian Academy of Sciences (MTA KFKI RMKI), H-1525 Budapest 114, PO Box 49, Budapest, Hungary
³¹Korea University, Seoul, 136-701, Korea
³²Russian Research Center “Kurchatov Institute”, Moscow, 123098 Russia
³³Kyoto University, Kyoto 606-8502, Japan
³⁴Laboratoire Leprince-Ringuet, Ecole Polytechnique, CNRS-IN2P3, Route de Saclay, F-91128, Palaiseau, France
³⁵Lawrence Livermore National Laboratory, Livermore, California 94550, USA
³⁶Los Alamos National Laboratory, Los Alamos, New Mexico 87545, USA
³⁷LPC, Université Blaise Pascal, CNRS-IN2P3, Clermont-Fd, 63177 Aubiere Cedex, France
³⁸Department of Physics, Lund University, Box 118, SE-221 00 Lund, Sweden
³⁹University of Maryland, College Park, Maryland 20742, USA
⁴⁰Department of Physics, University of Massachusetts, Amherst, Massachusetts 01003-9337, USA
⁴¹Institut für Kernphysik, University of Muenster, D-48149 Muenster, Germany
⁴²Muhlenberg College, Allentown, Pennsylvania 18104-5586, USA
⁴³Myongji University, Yongin, Kyonggido 449-728, Korea
⁴⁴Nagasaki Institute of Applied Science, Nagasaki-shi, Nagasaki 851-0193, Japan
⁴⁵University of New Mexico, Albuquerque, New Mexico 87131, USA
⁴⁶New Mexico State University, Las Cruces, New Mexico 88003, USA
⁴⁷Oak Ridge National Laboratory, Oak Ridge, Tennessee 37831, USA
⁴⁸IPN-Orsay, Université Paris Sud, CNRS-IN2P3, BP1, F-91406, Orsay, France
⁴⁹Peking University, Beijing 100871, P. R. China
⁵⁰PNPI, Petersburg Nuclear Physics Institute, Gatchina, Leningrad region, 188300, Russia
⁵¹RIKEN Nishina Center for Accelerator-Based Science, Wako, Saitama 351-0198, Japan
⁵²RIKEN BNL Research Center, Brookhaven National Laboratory, Upton, New York 11973-5000, USA
⁵³Physics Department, Rikkyo University, 3-34-1 Nishi-Ikebukuro, Toshima, Tokyo 171-8501, Japan
⁵⁴Saint Petersburg State Polytechnic University, St. Petersburg, 195251 Russia
⁵⁵Universidade de São Paulo, Instituto de Física, Caixa Postal 66318, São Paulo CEP05315-970, Brazil
⁵⁶Seoul National University, Seoul, Korea

⁵⁷Chemistry Department, Stony Brook University, SUNY, Stony Brook, New York 11794-3400, USA⁵⁸Department of Physics and Astronomy, Stony Brook University, SUNY, Stony Brook, New York 11794-3400, USA⁵⁹University of Tennessee, Knoxville, Tennessee 37996, USA⁶⁰Department of Physics, Tokyo Institute of Technology, Oh-okayama, Meguro, Tokyo 152-8551, Japan⁶¹Institute of Physics, University of Tsukuba, Tsukuba, Ibaraki 305, Japan⁶²Vanderbilt University, Nashville, Tennessee 37235, USA⁶³Waseda University, Advanced Research Institute for Science and Engineering, 17 Kikui-cho, Shinjuku-ku, Tokyo 162-0044, Japan⁶⁴Weizmann Institute, Rehovot 76100, Israel⁶⁵Yonsei University, IPAP, Seoul 120-749, Korea

(Received 22 May 2011; revised manuscript received 27 September 2011; published 14 December 2011)

Flow coefficients v_n for $n = 2, 3, 4$, characterizing the anisotropic collective flow in Au + Au collisions at $\sqrt{s_{NN}} = 200$ GeV, are measured relative to event planes Ψ_n , determined at large rapidity. We report v_n as a function of transverse momentum and collision centrality, and study the correlations among the event planes of different order n . The v_n are well described by hydrodynamic models which employ a Glauber Monte Carlo initial state geometry with fluctuations, providing additional constraining power on the interplay between initial conditions and the effects of viscosity as the system evolves. This new constraint can serve to improve the precision of the extracted shear viscosity to entropy density ratio η/s .

DOI: 10.1103/PhysRevLett.107.252301

PACS numbers: 25.75.Dw, 25.75.Ld

The production of particles in heavy ion collisions at the Relativistic Heavy Ion Collider is anisotropic in directions transverse to the beam. For low momentum particles ($p_T \lesssim 3$ GeV/ c), this anisotropy is understood to result from hydrodynamically driven flow of the quark-gluon plasma (QGP) [1–5]. The strength of the flow is measured as Fourier coefficients $v_n = \langle e^{in(\phi - \Psi_{RP})} \rangle$, $n = 2, 4, \dots$ where ϕ is the azimuthal angle of an emitted particle around the z axis defined by the beam; Ψ_{RP} is the azimuth of the reaction plane defined by the beam direction and the impact vector between the colliding nuclei. The brackets denote averaging over particles and events. The reaction plane is not measurable directly *a priori*, so the Fourier coefficients are determined with respect to the estimated participant event planes [1]. Earlier measurements have focused on the even-order anisotropies v_2 and v_4 , evaluated with respect to an event plane Ψ_2 , determined from the $n = 2$ correlation.

The $v_2(v_4)$ values obtained this way for a broad range of p_T and centrality have been used to extract the specific viscosity η/s (the ratio of shear viscosity η to entropy density s) of the hot and dense nuclear matter via hydrodynamic model comparisons [6–10]. These model comparisons, which incorporate the dynamic evolution of an early-stage strongly coupled QGP, together with a late-stage hadronic gas, show an ambiguity for very different values of $4\pi\eta/s \approx 2$ and $4\pi\eta/s \approx 1$, the latter being a conjectured lower bound for the specific viscosity [11]. Specifically the two values correspond to two equally successful parameter sets, each including different estimates of the initial state anisotropy (parameterized as “eccentricity” see below) [7,8,12], which dominate the associated uncertainty in these models. The lower bound value is obtained with a standard Glauber Monte Carlo (Glauber-MC) model [13,14] of the initial state which results in smaller initial elliptical eccentricity and thus

needs less viscosity to reproduce the measured final state particle anisotropy. The higher value $4\pi\eta/s \approx 2$, corresponds to a larger initial eccentricity in the color-glass condensate inspired Monte Carlo Kharzeev-Levin-Nardi (MC-KLN) model [15–17] of the initial state.

Recently, significant attention has been given to the study of the influence of initial geometry fluctuations of the initial state anisotropy [18] which are typically quantified by higher-order generalized “eccentricities” ε_n [18,19]. The goal has been to understand how such fluctuations induce anisotropic particle emission, characterized by v_n (for odd and even n)

$$\frac{dN}{d\phi} \propto 1 + \sum_{n=1} 2v_n \cos(n[\phi - \Psi_n]), \quad (1)$$

where $v_n = \langle \cos(n[\phi - \Psi_n]) \rangle$, $n = 1, 2, 3, \dots$ and the Ψ_n are the generalized participant event planes at all orders for each event. These recent developments suggest that measurements of v_n , especially for $n = 3$, can yield important additional constraints that provide a more precise estimate of $\frac{\eta}{s}$, as well as resolve the correct eccentricity model.

Here we present results for differential measurements following Eq. (1), for Au + Au collisions at $\sqrt{s_{NN}} = 200$ GeV. We first show how the measured event planes correlate across large rapidity gaps, and then show resulting v_n moments for midrapidity particles relative to those planes. The results are derived from $\sim 3.0 \times 10^9$ Au + Au events obtained with the PHENIX detector [20] during the 2007 running period. Collision centrality (related to impact parameter) and number of participating nucleons (N_{part}) are estimated as in [9] through comparisons of detected multiplicity in beam-beam counters (BBCs) [21] with a Glauber-MC calculation. Event planes were determined using three separate detector systems: the same BBCs, reaction-plane detectors (RXNs) [22], and muon-piston

calorimeters (MPCs). Each detector system has a north (south) component to measure at forward (backward) rapidity. The absolute pseudorapidity (η') coverages for these detectors are $3.1 < |\eta'_{\text{BBC}}| < 3.9$, $1.0 < |\eta'_{\text{RXN}}| < 2.8$, $3.1 < |\eta'_{\text{MPC}}| < 3.7$. The PHENIX drift and pad chambers [23] were used for charged particle tracking and momentum reconstruction with azimuthal angle coverage $\varphi = \pi$ rad in the central region ($|\eta'| \leq 0.35$).

To estimate the event plane Ψ_n in each detector, we generalize to all orders n our earlier procedure for event-plane determination (see [9] and especially definitions in [24]). For each event-plane detector we evaluate $\tan(n\Phi_n) = \sum w_i \sin(n\phi_i) / \sum w_i \cos(n\phi_i)$ for the Ψ_n sub-event estimator Φ_n , where the ϕ_i are the azimuths of elements in that detector and the weights w_i reflect the energy or multiplicity in that element. Acceptance corrections [24] for imperfect detector efficiency were employed to ensure a flat (azimuthally independent) event-plane distribution, as required by symmetry considerations. In general, the hit distributions sample virtually all momenta.

To measure v_n , the azimuth ϕ of each particle is correlated with the Ψ_n via Eq. (1). The measured $v_n\{\Psi_n\} = \langle \cos(n[\phi - \Phi_n^{\text{avg}}]) \rangle / \text{Res}(\Psi_n)$, where Φ_n^{avg} is the average of the Φ_n for north and south subevents and where the denominator $\text{Res}(\Psi_n)$ represents a resolution factor described in [24]. This factor corrects v_n for the event-by-event dispersion of the Φ_n . Its magnitude can be estimated via the two and three subevents method [9] in which the correlation between Φ_n from different subevents is measured. The strength of this correlation is generally quantified as $\langle \cos(n[\Phi_n^A - \Phi_n^B]) \rangle$ for subevents A, B , which measures the cosine of the dispersion of the Φ_n estimator with respect to the true Ψ_n .

Figure 1 shows the centrality dependence of this correlation strength $\langle \cos(j[\Phi_n^A - \Phi_m^B]) \rangle$ for subevent combinations (A, B) involving different event-plane detectors with $\Delta\eta' \sim 5$ and $\Delta\eta' \sim 7$. The raw correlations are presented as measured; however, the magnitudes are specific to the PHENIX detectors involved. The systematic uncertainties (not shown) for these correlations are of similar relative size to those for $v_n\{\Psi_n\}$ discussed below. The uncertainties are correlated across centrality and n such that the relative size of these event-plane correlations can be compared. The magnitudes for the odd parity quantities $\langle \sin(j[\Phi_n^A - \Phi_m^B]) \rangle$, which should vanish, are found to be consistent with zero for all centrality, j , and Φ combinations. Figure 1 panels (a) and (b) show the two subevent correlations for $m = n$; (c) and (d) show the two subevent correlations for $m \neq n$. The negative correlation indicated in (a) for $n = 1$ is due to the well-known antisymmetric pseudorapidity dependence (sign change about midrapidity) of sideways flow v_1 , as well as momentum conservation [2]. Positive subevent correlations are indicated in (a) and (b) for $\Psi_{2,3,4}$, with sizable magnitudes for $\Psi_{2,3}$ and much smaller values for Ψ_4 .

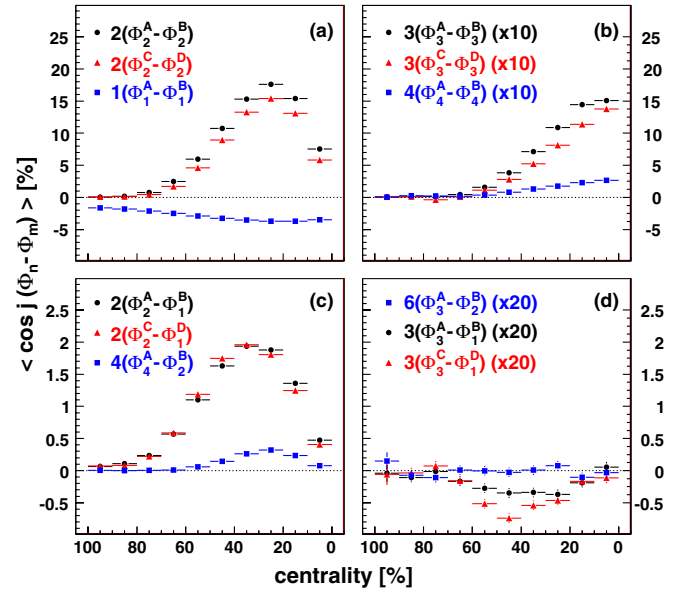


FIG. 1 (color online). Raw correlation strengths $\langle \cos(j[\Phi_n^A - \Phi_m^B]) \rangle$ and $\langle \cos(j[\Phi_n^C - \Phi_m^D]) \rangle$ of the event planes for various detector combinations as a function of the collision centrality, binned in percentages of the total cross section, where 0% corresponds to impact parameter = 0. Panels (a) and (b) show the two subevent correlations for $m = n$; (c) and (d) show the two subevent correlations for $m \neq n$. The detectors in which the event plane is measured are: A: RXN North, B: BBC South, C: MPC North, and D: MPC South. Data in (b) and (d) have been scaled by factors of 10 and 20, respectively.

The subevent correlations $\langle \cos(j[\Phi_n^A - \Phi_m^B]) \rangle$ for $n \neq m$ are also of interest. Figure 1(c) confirms the expected correlation between Ψ_1 and Ψ_2 (due to sideways flow), as well as that between Ψ_2 and Ψ_4 [24]. By contrast, Fig. 1(d) shows that there is no significant correlation observed between Ψ_2 and Ψ_3 , a result which is independent of the detectors used. The order $j = 6$ is chosen to account for the n multiplet of directions ($2\pi/n$) of Ψ_2 and Ψ_3 . The absence of this correlation suggests that the fluctuations for Ψ_3 about Ψ_2 are substantial. This is well reproduced by Glauber modeling [25,26] and therefore supports an initial state fluctuation origin of Ψ_3 and v_3 . A small correlation between Ψ_3 and Ψ_1 is indicated in Fig. 1(d). While such a correlation seems to be at odds with the absence of a $\Psi_2 - \Psi_3$ correlation [Fig. 1(d)], we note that $\Psi_1 - \Psi_3$ correlations need not contribute to a residual contribution to $\Psi_2 - \Psi_3$ correlations through Ψ_1 . That is, Ψ_1 could correlate with Ψ_3 and Ψ_2 in exclusive event classes. Correlations involving the PHENIX zero-degree calorimeter, which measures the $n = 1$ spectator neutron event plane [24] at $|\eta'| > 6.5$ indicate that this correlation has some degree of η' antisymmetry. We defer further investigation of these correlation subtleties to future work.

Figure 2 shows results for the midrapidity $v_n\{\Psi_n\}$ for tracks in the central arms as a function of p_T for different centralities. RXN-defined event planes, which have the

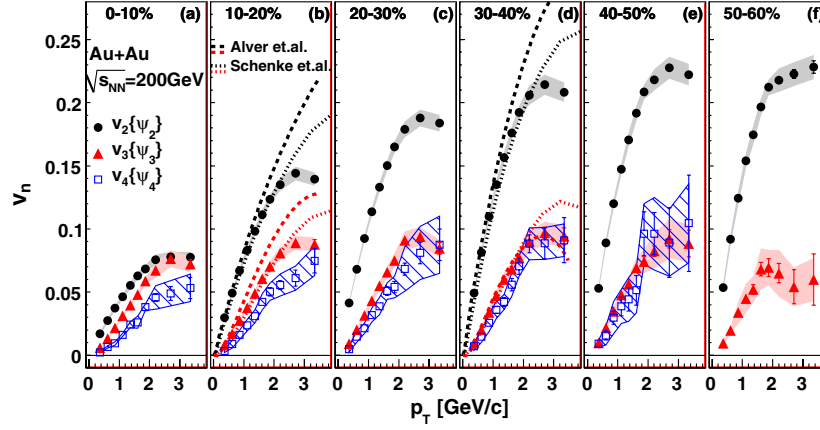


FIG. 2 (color online). $v_n\{\Psi_n\}$ vs p_T measured via the reaction-plane method for different centrality bins; 0%–10% are the most central collisions. Shaded (gray and pink) and hatched (blue) areas around the data points indicate sizes of systematic uncertainties. The curves in panels (b) and (d) are predictions for $v_2\{\Psi_2\}$ and $v_3\{\Psi_3\}$ from two hydrodynamic models, both using Glauber initial conditions and $4\pi\eta/s = 1$, Alver *et al.* [27] and Schenke *et al.* [32].

best resolution, are employed. The systematic uncertainties for these measurements were estimated by detailed comparisons of the results obtained with the RXN, BBC, and MPC event-plane detectors and subevent selections. They are $\sim 3\%$, $\sim 8\%$ and $\sim 20\%$ for $v_2\{\Psi_2\}$, $v_3\{\Psi_3\}$, and $v_4\{\Psi_4\}$, respectively, for midcentral collisions and increase by a few percent for more central and peripheral collisions. Through further comparison of the results obtained with the RXN, BBC, and MPC event-plane detectors, pseudorapidity dependent nonflow contributions that may influence the magnitude of $v_n\{\Psi_n\}$, such as jet correlations, were shown [9] to be much less than all other uncertainties for $v_2\{\Psi_2\}$ and $v_4\{\Psi_4\}$.

The $v_n\{\Psi_n\}$ values shown in Fig. 2 increase with p_T for most of the measured range, and decrease for more central collisions. The $v_2\{\Psi_2\}$ increases as expected from central to semiperipheral collisions, following the expected increase of ε_n with impact parameter [19,27,28]. The $v_3\{\Psi_3\}$ and, albeit with less statistical significance, also the $v_4\{\Psi_4\}$ appear to be much less centrality dependent, with v_3 values comparable to $v_2\{\Psi_2\}$ in the most central events. This behavior is consistent with Glauber calculations of the average fluctuations of the generalized “triangular” eccentricity ε_3 [25,26]. The Fig. 2 panels (b) and (d) show comparisons of $v_2\{\Psi_2\}$ and $v_3\{\Psi_3\}$ to results from hydrodynamic calculations. The p_T and centrality trends for both $v_2\{\Psi_2\}$ and $v_3\{\Psi_3\}$ are in good agreement with the hydrodynamic models shown, especially at p_T below ≈ 1 GeV/c.

Figure 3 compares the centrality dependence of $v_2\{\Psi_2\}$ and $v_3\{\Psi_3\}$ with several additional calculations, demonstrating both the new constraints the data provide and also the robustness of hydrodynamics to the details of different model assumptions for medium evolution. Alver *et al.* [27] use relativistic viscous hydrodynamics in 2 + 1 dimensions. Fluctuations are introduced for two different initial

conditions. For Glauber initial conditions, the energy density distribution in the transverse plane is proportional to a superposition of struck nucleon and binary-collision densities; in MC-KLN initial conditions the energy density profile is further controlled by the dependence of the gluon saturation momentum on the transverse position [16,17]. The Glauber-MC and MC-KLN initial state models are paired with the values $4\pi\eta/s = 1$ and 2, respectively, to reproduce the measured $v_2\{\Psi_2\}$ [8]. The viscosity difference compensates for the $\sim 20\%$ difference between the initial ε_2 values associated with each model. The two models have similar ε_3 , and thus the larger viscosity needed with MC-KLN calculations to match v_2 , leads to a much lower v_3 than obtained with Glauber MC calculations. Consequently, our measurement of $v_3\{\Psi_3\}$ helps to

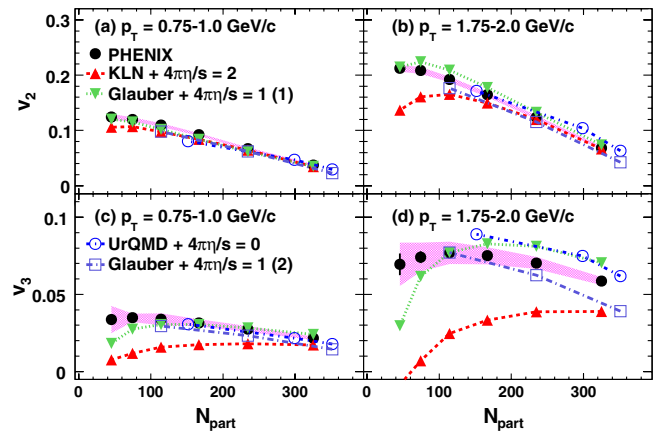


FIG. 3 (color online). Comparison of [(a) and (b)] $v_2\{\Psi_2\}$ vs N_{part} and [(c) and (d)] $v_3\{\Psi_3\}$ vs N_{part} measurements and theoretical predictions (see text): “MC-KLN + $4\pi\eta/s = 2$ ” and “Glauber + $4\pi\eta/s = 1$ (1)” [27]; “Glauber + $4\pi\eta/s = 1$ (2)” [32]; and “UrQMD” [29]. Shaded areas (magenta) around the data points indicate sizes of systematic uncertainties.

disentangle viscosity and initial conditions. The efficacy of these $2 + 1$ hydrodynamic results for Glauber initial conditions are confirmed by further calculations with different model assumptions. Petersen *et al.* [29] determine a Glauber initial state event by event, translating through preequilibrium with the UrQMD transport model [30,31], then evolving the medium with ideal QGP hydrodynamics ($\eta/s = 0$), and finally switching to a hadronic cascade (which has an effective viscosity) as regions become dilute. B. Schenke *et al.* [32] use event-by-event Glauber initial conditions, evolved with relativistic viscous $3 + 1$ dimensional hydrodynamics with $4\pi\eta/s = 1$.

All of these models are compared with $v_2\{\Psi_2\}$, and $v_3\{\Psi_3\}$ data as a function of N_{part} in two p_T bins. All calculations describe $v_2\{\Psi_2\}$ well at $p_T = 0.75$ GeV/ c . Deviations from hydrodynamics should be expected in peripheral collisions, where nonequilibrium effects may be large. At higher p_T , differences between the calculations become more apparent. All models still agree with $v_2\{\Psi_2\}$, including MC-KLN initial conditions. However, the lower panels of Fig. 3 show the constraining power of $v_3\{\Psi_3\}$ and that the calculated results from viscous hydrodynamics, with MC-KLN initial conditions and $4\pi\eta/s = 2$, lie significantly below the data. This is more apparent in the higher p_T bin, even in the most central collisions. Therefore, our comparisons suggest that the combination of the current implementation of the MC-KLN initial conditions in concert with $4\pi\eta/s = 2$ is disfavored by our new $v_3\{\Psi_3\}$ measurements. This may suggest that the MC-KLN implementation or its application needs to be reevaluated (see [33]), but it does not necessarily imply that a color-glass condensate initial state is disfavored.

The results from the hydrodynamical calculations which employ Glauber initial condition fluctuations and $4\pi\eta/s = 1$ show relatively good agreement with the $v_{2,3}\{\Psi_{2,3}\}$ data. The exact statistical significance of these constraints should be determined through a global fit procedure, including a quantitative accounting of the breakdown of hydrodynamics in peripheral collisions, as well as of the systematics associated with the averaging of eccentricity fluctuations within the models. From our data it is already clear that the higher-order moment v_3 should provide an important avenue for constraining different physical properties of the QGP.

In summary, we have presented participant event-plane Ψ_n correlations and differential measurements of $v_n\{\Psi_n\}$ for $n = 2, 3, 4$ for charged hadrons using the generalized event-plane method. The higher-order harmonic moments $v_3\{\Psi_3\}$ and $v_4\{\Psi_4\}$ and the nonzero correlations between higher-order event planes across a large rapidity gap of $\Delta\eta' \gtrsim 7$, indicate that the initial state has transverse geometry fluctuations. These fluctuations affect the generalized eccentricities, which are subsequently propagated in the hydrodynamic evolution of the plasma. The evidence, includes (1) a lack of correlation between the measured

event planes of order $n = 2$ and 3 as predicted by Glauber modeling, assuming correlations of the event planes with the generalized eccentricity, (2) proper description of the shapes of the p_T dependence in the low p_T region by hydrodynamic calculations, and (3) agreement with several different initial state + hydrodynamic models across centralities for order $v_n\{\Psi_n\}$. The combined results for $v_{2,3}\{\Psi_{2,3}\}$, together with initial hydrodynamic-model calculations now suggest that one of the important factors contributing to a large uncertainty in the extracted value of $4\pi\eta/s$ can be significantly reduced. For the limited set of models considered, $4\pi\eta/s \approx 1$ is favored.

We thank the staff of the Collider-Accelerator and Physics Departments at Brookhaven National Laboratory and the staff of the other PHENIX participating institutions for their vital contributions. We acknowledge support from the Office of Nuclear Physics in the Office of Science of the Department of Energy, the National Science Foundation, Abilene Christian University Research Council, Research Foundation of SUNY, and Dean of the College of Arts and Sciences, Vanderbilt University (U.S.A), Ministry of Education, Culture, Sports, Science, and Technology and the Japan Society for the Promotion of Science (Japan), Conselho Nacional de Desenvolvimento Científico e Tecnológico and Fundação de Amparo à Pesquisa do Estado de São Paulo (Brazil), Natural Science Foundation of China (P.R. China), Ministry of Education, Youth and Sports (Czech Republic), Centre National de la Recherche Scientifique, Commissariat à l'Énergie Atomique, and Institut National de Physique Nucléaire et de Physique des Particules (France), Ministry of Industry, Science and Technologies, Bundesministerium für Bildung und Forschung, Deutscher Akademischer Austausch Dienst, and Alexander von Humboldt Stiftung (Germany), Hungarian National Science Fund, OTKA (Hungary), Department of Atomic Energy and Department of Science and Technology (India), Israel Science Foundation (Israel), National Research Foundation and WCU program of the Ministry Education Science and Technology (Korea), Ministry of Education and Science, Russian Academy of Sciences, Federal Agency of Atomic Energy (Russia), VR and the Wallenberg Foundation (Sweden), the U.S. Civilian Research and Development Foundation for the Independent States of the Former Soviet Union, the US-Hungarian Fulbright Foundation for Educational Exchange, and the US-Israel Binational Science Foundation.

*Deceased

†PHENIX Spokesperson.

jacak@skipper.physics.sunysb.edu

[1] J.-Y. Ollitrault, *Phys. Rev. D* **46**, 229 (1992).

[2] U. Heinz and P. Kolb, *Nucl. Phys. A* **702**, 269 (2002).

- [3] E. Shuryak, *Prog. Part. Nucl. Phys.* **62**, 48 (2009).
- [4] K. Adcox *et al.* (PHENIX Collaboration), *Nucl. Phys. A* **757**, 184 (2005).
- [5] J. Adams *et al.* (STAR Collaboration), *Nucl. Phys. A* **757**, 102 (2005).
- [6] P. Romatschke and U. Romatschke, *Phys. Rev. Lett.* **99**, 172301 (2007).
- [7] T. Hirano and Y. Nara, *Phys. Rev. C* **79**, 064904 (2009).
- [8] H. Song *et al.*, *Phys. Rev. Lett.* **106**, 192301 (2011).
- [9] A. Adare *et al.* (PHENIX Collaboration), *Phys. Rev. Lett.* **105**, 062301 (2010).
- [10] C. Gombeaud and J.-Y. Ollitrault, *Phys. Rev. C* **81**, 014901 (2010).
- [11] P. K. Kovtun, D. T. Son, and A. O. Starinets, *Phys. Rev. Lett.* **94**, 111601 (2005).
- [12] R. A. Lacey *et al.*, *Phys. Rev. C* **82**, 034910 (2010).
- [13] M. Miller *et al.*, *Annu. Rev. Nucl. Part. Sci.* **57**, 205 (2007).
- [14] B. Alver *et al.* (PHOBOS Collaboration), *Phys. Rev. Lett.* **98**, 242302 (2007).
- [15] D. Kharzeev and M. Nardi, *Phys. Lett. B* **507**, 121 (2001).
- [16] T. Lappi and R. Venugopalan, *Phys. Rev. C* **74**, 054905 (2006).
- [17] H.-J. Drescher and Y. Nara, *Phys. Rev. C* **76**, 041903 (2007).
- [18] B. Alver and G. Roland, *Phys. Rev. C* **81**, 054905 (2010).
- [19] R. A. Lacey *et al.*, *Phys. Rev. C* **83**, 044902 (2011).
- [20] K. Adcox *et al.* (PHENIX Collaboration), *Nucl. Instrum. Methods Phys. Res., Sect. A* **499**, 469 (2003).
- [21] M. Allen *et al.* (PHENIX Collaboration), *Nucl. Instrum. Methods Phys. Res., Sect. A* **499**, 549 (2003).
- [22] E. Richardson *et al.* (PHENIX Collaboration), *Nucl. Instrum. Methods Phys. Res., Sect. A* **636**, 99 (2011).
- [23] K. Adcox *et al.* (PHENIX Collaboration), *Nucl. Instrum. Methods Phys. Res., Sect. A* **499**, 489 (2003).
- [24] S. Afanasiev *et al.* (PHENIX Collaboration), *Phys. Rev. C* **80**, 024909 (2009).
- [25] J. L. Nagle and M. P. McCumber, *Phys. Rev. C* **83**, 044908 (2011).
- [26] R. A. Lacey *et al.*, *Phys. Rev. C* **84**, 027901 (2011).
- [27] B. H. Alver, C. Gombeaud, M. Luzum, and J.-Y. Ollitrault, *Phys. Rev. C* **82**, 034913 (2010).
- [28] P. Staig and E. Shuryak, [arXiv:1008.3139v2](https://arxiv.org/abs/1008.3139v2).
- [29] H. Petersen, G. Y. Qin, S. A. Bass, and B. Muller, *Phys. Rev. C* **82**, 041901 (2010).
- [30] S. A. Bass *et al.*, *Prog. Part. Nucl. Phys.* **41**, 255 (1998).
- [31] M. Bleicher *et al.*, *J. Phys. G* **25**, 1859 (1999).
- [32] B. Schenke, S. Jeon, and C. Gale, *Phys. Rev. Lett.* **106**, 042301 (2011).
- [33] J. L. Albacete, A. Dumitru, and Y. Nara, [arXiv:1106.0978](https://arxiv.org/abs/1106.0978).